

Is minimising the convergence rate a good choice for efficient Optimized Schwarz preconditioning in heterogeneous coupling? The Stokes-Darcy case

Marco Discacciati and Luca Gerardo-Giorda

Abstract Optimized Schwarz Methods (OSM) are domain decomposition techniques based on Robin-type interface condition that have become increasingly popular in the last two decades. Ensuring convergence also on non-overlapping decompositions, OSM are naturally advocated for the heterogeneous coupling of multi-physics problems. Classical approaches optimize the coefficients in the Robin condition by minimizing the effective convergence rate of the resulting iterative algorithm. However, when OSM are used as preconditioners for Krylov solvers of the resulting interface problem, such parameter optimization does not necessarily guarantee the fastest convergence. This drawback is already known for homogeneous decomposition, but in the case of heterogeneous decomposition, the poor performance of the classical optimization approach becomes utterly evident. In this paper, we highlight this drawback for the Stokes/Darcy problem and propose a more effective optimization procedure.

1 Problem settings

The Stokes-Darcy problem, a classical model for the filtration of an incompressible fluid in a porous media [2], is a good example of a multi-physics problem where two different boundary value problems are coupled into a global heterogeneous one.

The problem is defined on a bounded domain $\Omega \subset \mathbb{R}^D$ ($D = 2, 3$) formed by two non overlapping subregions: the fluid domain Ω_f and the porous medium Ω_p separated by an interface Γ . If the fluid is incompressible with constant viscosity and density, and low Reynolds' number, it can be described by the Stokes equations

Marco Discacciati

Department of Mathematical Sciences, Loughborough University, LE11 3TU, Loughborough UK,
e-mail: m.discacciati@lboro.ac.uk

Luca Gerardo-Giorda

BCAM - Basque Center for Applied Mathematics, Bilbao, Spain, e-mail: lgerardo@bcamath.org

in Ω_f and by Darcy's law in Ω_p . The physics of the problem naturally drives the decomposition of the domain and, at the same time, imposes interface conditions across Γ to describe filtration phenomena. The coupled problem reads as follows: Find the fluid velocity \mathbf{u}_f and pressure p_f , and the pressure p_p such that

$$\begin{aligned}
-\nabla \cdot \boldsymbol{\sigma}(\mathbf{u}_f, p_f) &= \mathbf{f}_f && \text{in } \Omega_f && \text{Stokes equations} \\
\nabla \cdot \mathbf{u}_f &= 0 && \text{in } \Omega_f && \\
-\nabla \cdot (\eta_p \nabla p_p) &= g_p && \text{in } \Omega_p && \text{Darcy's equation} \\
-(\eta_p \nabla p_p) \cdot \mathbf{n} &= \mathbf{u}_f \cdot \mathbf{n} && \text{on } \Gamma && \text{continuity of the normal velocity} \\
-\mathbf{n} \cdot \boldsymbol{\sigma}(\mathbf{u}_f, p_f) \cdot \mathbf{n} &= p_p && \text{on } \Gamma && \text{continuity of the normal stresses} \\
-\boldsymbol{\tau} \cdot \boldsymbol{\sigma}(\mathbf{u}_f, p_f) \cdot \mathbf{n} &= \xi \mathbf{u}_f \cdot \boldsymbol{\tau} && \text{on } \Gamma && \text{BJS condition on the tangential stresses}
\end{aligned} \tag{1}$$

where $\boldsymbol{\sigma}(\mathbf{u}_f, p_f) = \mu_f(\nabla \mathbf{u}_f + (\nabla \mathbf{u}_f)^T) - p_f I$ is the Cauchy stress tensor, while \mathbf{f}_f and g_p are given external forces. The Beaver-Joseph-Saffman (BJS, [1]) condition does not play any role in the coupling of the local problems. Thus, coupling on Γ can be obtained by linear combination of the first two conditions:

$$\begin{aligned}
-\mathbf{n} \cdot \boldsymbol{\sigma}(\mathbf{u}_f, p_f) \cdot \mathbf{n} - \alpha_f \mathbf{u}_f \cdot \mathbf{n} &= p_p + \alpha_f (\eta_p \nabla p_p) \cdot \mathbf{n} \\
p_p - \alpha_p (\eta_p \nabla p_p) \cdot \mathbf{n} &= -\mathbf{n} \cdot \boldsymbol{\sigma}(\mathbf{u}_f, p_f) \cdot \mathbf{n} + \alpha_p \mathbf{u}_f \cdot \mathbf{n}
\end{aligned} \tag{2}$$

Using the interface conditions (2) a Robin-Robin method can be formulated. Such method requires solving iteratively the Stokes problem in Ω_f with boundary condition (2)₁ on Γ and Darcy's equation in Ω_p with boundary condition (2)₂ on Γ . More details can be found in [3].

2 Optimization of the Robin parameters α_p and α_f

Classical approaches in the Optimized Schwarz literature derive, through Fourier analysis, the convergence rate $\rho(\alpha_f, \alpha_p, k)$ of the iterative algorithm as a function of the parameters α_f , α_p and of the frequency k , and they aim at optimizing α_f and α_p by minimization of $\rho(\alpha_f, \alpha_p, k)$ over all the relevant frequencies of the problem. This amounts to solve the min-max problem

$$\min_{\alpha_f, \alpha_p \in \mathbb{R}^+} \max_{k \in [k_{min}, k_{max}]} \rho(\alpha_f, \alpha_p, k), \tag{3}$$

where k_{min} and k_{max} are the minimal frequency relevant to the problem and the maximal frequency supported by the numerical grid (of the order of π/h).

However, when the OSM is used as a preconditioner for a Krylov method to solve the interface problem, such a choice does not necessarily guarantee the fastest convergence. Minimising the effective convergence rate ($\rho_{eff}(\alpha_f, \alpha_p) = \max_k \rho(\alpha_f, \alpha_p, k)$) does not make the convergence rate automatically small for all frequencies, and the Krylov type solver can then suffer from slow convergence. Such an issue can be particularly relevant in the presence of heterogeneous cou-

pling. In the rest of the section, we first introduce the exact interface conditions, then present three different approaches to optimize the interface parameters. The first one is based on a classical equioscillation principle, the second one exploits the peculiar characteristics of the Stokes/Darcy problem, while the third one aims to globally minimize the convergence rate for all frequencies.

2.1 Convergence rate and exact interface conditions

The convergence rate of the Robin-Robin algorithm does not depend on the iteration and, for positive parameters $\alpha_p, \alpha_f > 0$, is given by [3]

$$\rho(\alpha_f, \alpha_p, k) = \left| \frac{2\mu_f k - \alpha_p}{2\mu_f k + \alpha_f} \right| \cdot \left| \frac{1 - \alpha_f \eta_p k}{1 + \alpha_p \eta_p k} \right|. \quad (4)$$

(As shown in [3], by symmetry we can restrict to the case $k > 0$.)

The optimal parameters force the reduction factor $\rho(\alpha_f, \alpha_p, k)$ to be identically equal to zero for all k , so that convergence is attained in a number of iterations equal to the number of subdomains. They can be easily derived from (4) as

$$\alpha_p^{exact}(k) = 2\mu_f k \quad \alpha_f^{exact}(k) = \frac{1}{\eta_p k}. \quad (5)$$

Their direct use is unfortunately not viable: both depend on the frequency k , and their back transforms in the physical space are either introducing an imaginary coefficient which multiplies a first order tangential derivative ($\alpha_p^{exact}(k)$) or result in a nonlocal operator ($\alpha_f^{exact}(k)$). The use of approximations based on low-order Taylor expansions of the optimal values (5) (around $k = k_{min}$ for α_p and $k = k_{max}$ for α_f) would not help either, as they would suffer from the same drawbacks (see [3]).

2.2 The equioscillation approach

The convergence rate (4) is continuous, has two positive roots, $k_1 = (\alpha_f \eta_p)^{-1}$ and $k_2 = \alpha_p / (2\mu_f)$, and a maximum between k_1 and k_2 , given by (setting $\delta = 2\mu_f \eta_p$)

$$k_* = \frac{2\delta(\alpha_p - \alpha_f) + \sqrt{4\delta^2(\alpha_p - \alpha_f)^2 + 4\delta(2\mu_s + \alpha_f \alpha_p \eta_p)^2}}{2\delta(2\mu_s + \alpha_f \alpha_p \eta_p)}. \quad (6)$$

The natural approach to solve the min-max problem (3) would resort to an equioscillation principle, where one seeks for α_f^{eq} and α_p^{eq} such that

$$\rho(\alpha_f^{eq}, \alpha_p^{eq}, k_{min}) = \rho(\alpha_f^{eq}, \alpha_p^{eq}, k_*) = \rho(\alpha_f^{eq}, \alpha_p^{eq}, k_{max}). \quad (7)$$

This approach ensures that all other frequencies exhibit a smaller convergence rate.

Proposition 1. *The solution to problem (7) is given by the two pairs of optimal coefficients $(\alpha_{f,i}^{eq}, \alpha_{p,i}^{eq})$, $i = 1, 2$:*

$$\alpha_{f,i}^{eq} = \frac{1}{2} \left(X_i + \sqrt{X_i^2 + 4Y_i} \right), \quad \alpha_{p,i}^{eq} = \frac{1}{2} \left(-X_i + \sqrt{X_i^2 + 4Y_i} \right), \quad i = 1, 2, \quad (8)$$

with $Y_i \in \mathbb{R}^+$ and $X_i \in \mathbb{R}$ defined as follows:

$$Y_i = \frac{2\mu_f}{\eta_p} \left(\frac{b}{a} - 1 + (-1)^{i+1} \sqrt{\left(\frac{b}{a} - 1 \right)^2 - 1} \right) \quad i = 1, 2, \quad (9)$$

$$X_i = \frac{1 - \delta k_{min} k_{max}}{\eta_p (k_{min} + k_{max})} \left(\frac{\eta_p}{2\mu_f} Y_i + 1 \right) \quad i = 1, 2, \quad (10)$$

where $a > 0$ and $b > 0$ are the positive quantities

$$a = \frac{1 + \delta k_{max}^2}{(k_{min} + k_{max})^2} (k_{min}(k_* + k_{max}) + k_*(k_{max} - k_*)) + \delta k_{min} k_{max} (k_*(k_{min} + k_*) + k_{max}(k_* - k_{min})), \quad (11)$$

$$b = (1 + \delta k_{max}^2)(1 + \delta k_*^2), \quad (12)$$

and $k_* > 0$ becomes

$$k_* = \frac{\delta k_{min} k_{max} - 1 + \sqrt{(\delta k_{min} k_{max} - 1)^2 + \delta (k_{min} + k_{max})^2}}{\delta (k_{min} + k_{max})}. \quad (13)$$

Proof. We consider the first condition of equioscillation in (7): $\rho(\alpha_f, \alpha_p, k_{min}) = \rho(\alpha_f, \alpha_p, k_{max})$. With the help of some algebra, we obtain

$$\alpha_p - \alpha_f = (\delta k_{min} k_{max} - 1)(\eta_p \alpha_f \alpha_p + 2\mu_f)(\delta(k_{min} + k_{max}))^{-1}. \quad (14)$$

Substituting (14) into (6) we obtain the expression (13) for k_* which is now independent of α_f and α_p . It can be easily verified that the obtained value of k_* satisfies $k_{min} < k_* < k_{max}$ so that we can proceed imposing the second condition of equioscillation in (7): $\rho(\alpha_f, \alpha_p, k_{max}) = \rho(\alpha_f, \alpha_p, k_*)$, that is:

$$\begin{aligned} & -\delta(k_*^2 + k_{max}^2)(\alpha_f - \alpha_p)^2 + 2\eta_p k_* k_{max} (\alpha_f \alpha_p)^2 \\ & + \eta_p (k_* + k_{max})(1 - \delta k_* k_{max})(\alpha_f - \alpha_p) \alpha_f \alpha_p \\ & + 2\mu_f (k_* + k_{max})(1 - \delta k_* k_{max})(\alpha_f - \alpha_p) \\ & - 2(1 + \delta^2 k_*^2 k_{max}^2 + \delta(k_{max} - k_*)^2) \alpha_f \alpha_p + 8\mu_f^2 k_* k_{max} = 0. \end{aligned} \quad (15)$$

We introduce now the change of variables: $X = \alpha_f - \alpha_p$ and $Y = \alpha_f \alpha_p$. We substitute the expression of X from (14) into (15) to get

$$Y^2 \left(a \frac{\eta_p}{2\mu_f} \right) + 2Y(a-b) + a \frac{2\mu_f}{\eta_p} = 0 \quad (16)$$

where a and b are as in (11) and (12), respectively. Since $k_{min} < k_* < k_{max}$, $a > 0$ and we can rewrite (16) as

$$Y^2 \frac{\eta_p}{2\mu_f} - 2Y \left(\frac{b}{a} - 1 \right) + \frac{2\mu_f}{\eta_p} = 0 \quad (17)$$

whose roots are (9). By a simple algebraic manipulation, it can be verified that $b - 2a > 0$ which also implies that $b - a > 0$, so that the discriminant of (17) is positive and both its roots are positive as well: $Y_i > 0$, $i = 1, 2$. Finally, (10) follows from (14) and (8) is obtained reversing the change of variables. \square

2.3 Exploiting the problem characteristics

From (5), we observe that the product of the optimal values $\alpha_f^{exact}(k)$ and $\alpha_p^{exact}(k)$ is constant and equals $2\mu_f/\eta_p$. We exploit such peculiarity of the problem (not occurring in homogeneous decomposition, see e.g. [5]), and restrict our search for optimized parameters to the curve

$$\alpha_f \alpha_p = 2\mu_f/\eta_p. \quad (18)$$

Notice that such curve is the subset of the (α_f, α_p) upper-quadrant where the zeros k_1 and k_2 of the convergence rate ρ coincide.

Proposition 2 ([3]). *The solution of the min-max problem*

$$\min_{\alpha_f \alpha_p = \frac{2\mu_f}{\eta_p}} \max_{k \in [k_{min}, k_{max}]} \rho(\alpha_f, \alpha_p, k)$$

is given by the pair

$$\begin{aligned} \alpha_f^* &= \frac{1 - 2\mu_f \eta_p k_{min} k_{max}}{\eta_p (k_{min} + k_{max})} + \sqrt{\left(\frac{1 - 2\mu_f \eta_p k_{min} k_{max}}{\eta_p (k_{min} + k_{max})} \right)^2 + \frac{2\mu_f}{\eta_p}} \\ \alpha_p^* &= -\frac{1 - 2\mu_f \eta_p k_{min} k_{max}}{\eta_p (k_{min} + k_{max})} + \sqrt{\left(\frac{1 - 2\mu_f \eta_p k_{min} k_{max}}{\eta_p (k_{min} + k_{max})} \right)^2 + \frac{2\mu_f}{\eta_p}} \end{aligned} \quad (19)$$

Moreover, $\rho(\alpha_f^*, \alpha_p^*, k) < 1$ for all $k \in [k_{min}, k_{max}]$.

2.4 Minimisation of the mean convergence rate

The reduction factor along (18) is given by

$$\rho(\alpha_f, k) = \frac{2\mu_f}{\eta_p} \left(\frac{\eta_p \alpha_f k - 1}{2\mu_f k + \alpha_f} \right)^2. \quad (20)$$

To further exploit the characteristics of the problem, we consider the set

$$\mathcal{A}_f = \{\alpha_f > 0 : \rho(\alpha_f, k) \leq 1 \quad \forall k \in [k_{min}, k_{max}]\}.$$

Notice that the convergence of the Robin-Robin method in the iterative form would be ensured only if the inequality in the definition of \mathcal{A}_f is strict. From [3] we know that the convergence rate can equal 1 in at most one frequency, either in k_{min} or in k_{max} . When using the OSM as a preconditioner for a Krylov method, the latter can handle isolated problems in the spectrum (see, e.g., [4, 6, 7]).

In order to improve the overall convergence for a Krylov method, we minimize, on the set \mathcal{A}_f , the expected value of $\rho(\alpha_f, k)$ in the interval $[k_{min}, k_{max}]$:

$$E(\alpha_f) := \mathbb{E}[\rho(\alpha_f, k)] = \frac{1}{k_{max} - k_{min}} \int_{k_{min}}^{k_{max}} \rho(\alpha_f, k) dk.$$

Owing to (20), $E(\alpha_f)$ can be explicitly computed: it is positive in $\alpha_f = 0$, and has a minimum in the point $\hat{\alpha}_f$ after which it is always increasing (see [3]). As a consequence, the minimum α_f^{opt} of $E(\alpha_f)$ is attained in $\hat{\alpha}_f$ if the latter belongs to \mathcal{A}_f , or in one extremum of \mathcal{A}_f otherwise, namely:

$$\alpha_f^{opt} = \begin{cases} \min_{\alpha_f \in \mathcal{A}_f} \alpha_f & \text{if } \hat{\alpha}_f < \min_{\alpha_f \in \mathcal{A}_f} \alpha_f \\ \hat{\alpha}_f & \text{if } \hat{\alpha}_f \in \mathcal{A}_f \\ \max_{\alpha_f \in \mathcal{A}_f} \alpha_f & \text{if } \hat{\alpha}_f > \max_{\alpha_f \in \mathcal{A}_f} \alpha_f. \end{cases} \quad (21)$$

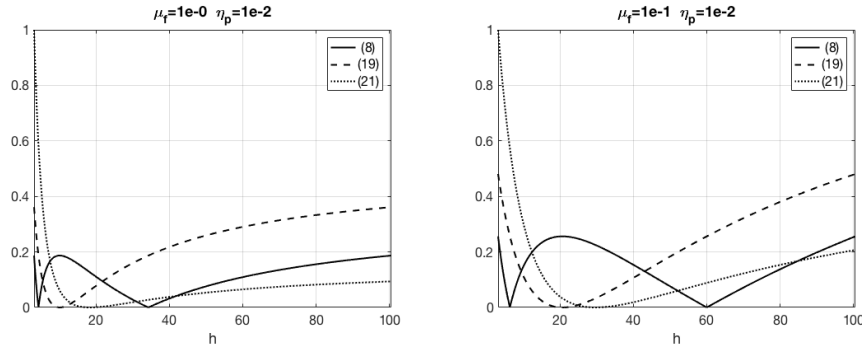
3 Numerical results

We compare here the three approaches (8), (19) and (21) considering a test with analytic solution: $\mathbf{u}_f = (\sqrt{\mu_f \eta_p}, \alpha_{BJ} x)$, $p_f = 2\mu_f(x + y - 1) + (3\eta_p)^{-1}$, $p_p = (-\alpha_{BJ} x(y - 1) + y^3/3 - y^2 + y)/\eta_p + 2\mu_f x$. We set $\Omega_f = (0, 1) \times (1, 2)$, $\Omega_p = (0, 1) \times (0, 1)$ and interface $\Gamma = (0, 1) \times \{1\}$. The computational grids are uniform, structured, made of triangles with $h = 2^{-(s+2)}$, $s \geq 0$; \mathbb{P}_2 - \mathbb{P}_1 finite elements are used for Stokes and \mathbb{P}_2 elements for Darcy's law; η_p is constant, $\alpha_{BJ} = 1$, $k_{min} = \pi$, $k_{max} = \pi/h$. The interface system associated to the OSM [3] is solved by GMRES with tolerance 1e-9. In Table 1 we report the parameters obtained for various coefficients μ_f and η_p . Figure 1 shows the convergence rates versus k for the three possible choices of α_f and α_p and two pairs of values (μ_f, η_p) . The number of iterations for α_f and α_p at fixed h is computed for two pairs of values (μ_f, η_p) and is

Table 1 Parameters obtained in (8), (19) and (21) for different values of μ_f , η_p and $h = 2^{-5}$.

| μ_f | η_p | α_f^{eq} | α_p^{eq} | α_f^* | α_p^* | α_f^{opt} | α_p^{opt} |
|---------|----------|-----------------|-----------------|--------------|--------------|------------------|------------------|
| 1 | 1 | 0.27 | 36.93 | 0.16 | 12.33 | 0.036 | 56.04 |
| 1 | 1e-2 | 23.00 | 68.59 | 9.91 | 20.17 | 5.44 | 36.75 |
| 1 | 1e-4 | 852.50 | 157.10 | 258.19 | 77.46 | 217.34 | 92.01 |
| 1e-1 | 1 | 0.26 | 4.19 | 0.15 | 1.35 | 0.03 | 5.48 |
| 1e-1 | 1e-2 | 15.71 | 12.01 | 4.84 | 4.13 | 3.37 | 5.93 |
| 1e-1 | 1e-4 | 613.00 | 17.02 | 201.61 | 9.92 | 195.90 | 10.21 |

shown in Figure 2. The parameters devised in (8) feature both the smallest convergence rate and the worst preconditioning performance in terms of iteration counts. Notice also that α_f^{opt} in (21), minimizing the mean convergence rate, always ensures the best performance in terms of iteration counts. Figure 3 displays the number of iterations versus h for different combinations of μ_f and η_p : α_f^{opt} consistently exhibits the best convergence properties, in particular when the ratio μ_f/η_p increases.


Fig. 1 Convergence rates as a function of k for the parameters (8) (solid line), (19) (dashed line), and (21) (dotted line). Left: $\mu_f = 1$, $\eta_p = 1e-2$. Right: $\mu_f = 1e-1$, $\eta_p = 1e-2$. $h = 2^{-5}$.

4 Conclusions

Using the Stokes/Darcy coupling as a testbed for heterogeneous problems, we show that minimizing the convergence rate of the corresponding iterative algorithm leads to poor convergence when an Optimized Schwarz Method is used as preconditioner for a Krylov method applied to the interface equation. On the other hand, taking advantage of the problem characteristics and minimizing the mean of the convergence rate provides effective preconditioning.

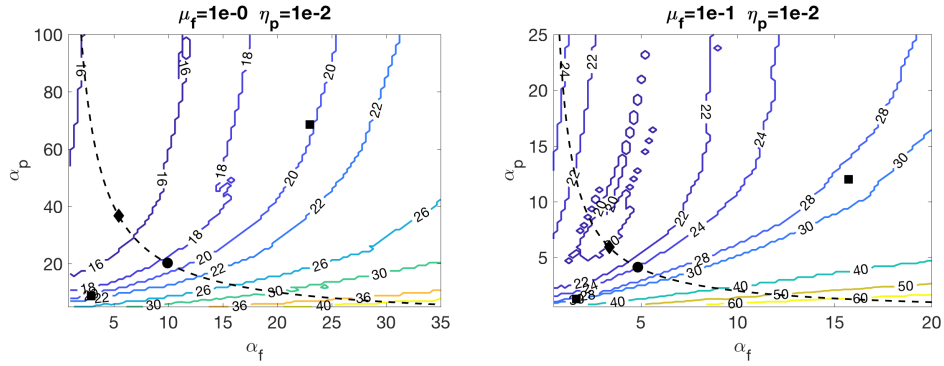


Fig. 2 Number of iterations for $h = 2^{-5}$ and parameters α_f and α_p as in (8) (squares), (19) (circle) and (21) (diamond). Left: $\mu_f = 1$, $\eta_p = 1e-2$; right: $\mu_f = 1e-1$, $\eta_p = 1e-2$.

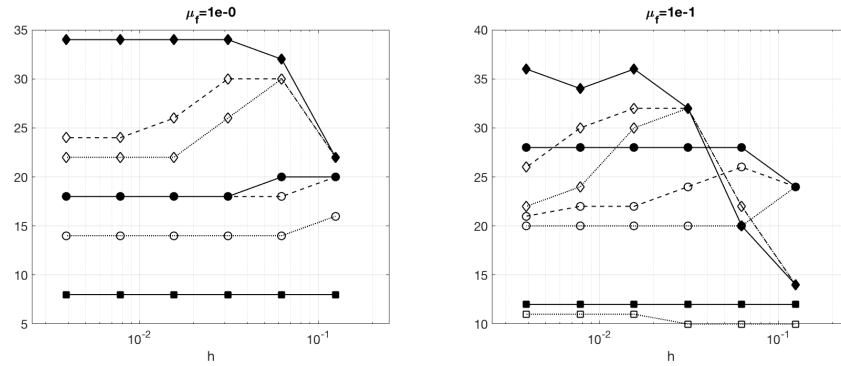


Fig. 3 Number of iterations versus h . Solid lines refer to (8), dashed lines to (19) and dotted lines (21). Squares refer to $\eta_p = 1$, circles $\eta_p = 1e-2$, diamonds $\eta_p = 1e-4$. Left: $\mu_f = 1$; right: $\mu_f = 1e-1$. All values obtained for $\eta_p = 1$ and $\mu_f = 1$ coincide (left plot), while for $\eta_p = 1$ and $\mu_f = 1e-1$ they coincide only when computed using (8) and (19) (right plot).

Acknowledgements

The second author was partly supported by the Basque government through the BERC 2014-2017, the Spanish Ministry of Economics and Competitiveness MINECO through the BCAM Severo Ochoa Excellence Accreditation SEV-2013-0323 and the Plan Estatal de Investigación. Desarrollo e Innovación Orientada a los Retos de la Sociedad under Grant BELEMET (MTM2015-69992-R)

References

1. G. Beavers and D. Joseph (1967) Boundary conditions at a naturally permeable wall. *J. Fluid*

- Mech.*, **30**, 197–207.
2. M. Discacciati and A. Quarteroni (2009) Navier-Stokes/Darcy coupling: modeling, analysis, and numerical approximation. *Rev. Mat. Complut.*, **22**, 315–426.
 3. M. Discacciati and L. Gerardo-Giorda (2017) Optimized Schwarz Methods for the Stokes-Darcy coupling *IMA J. Num. Anal.*, (submitted)
 4. V. Dolean, M.J. Gander, and L. Gerardo-Giorda (2009) Optimized Schwarz methods for Maxwell's equations. *SIAM J. Sci. Comput.*, **31**, 2193–2213.
 5. M.J. Gander. Optimized Schwarz methods. *SIAM J. Num. Anal.*, 44(2), pp. 699–731, 2006.
 6. M.J. Gander, F. Magoulès, and F. Nataf (2002) Optimized Schwarz methods without overlap for the Helmholtz equation. *SIAM J. Sci. Comput.*, **21**, 38–60.
 7. L. Gerardo-Giorda and M. Perego (2013) Optimized Schwarz methods for the Bidomain system in electrocardiology. *M2AN*, **75**, 583–608.